

Characterization of Single and Pairwise NO₂ Adsorption on the (MgO)₉ and (CaO)₉ Clusters

¹FATHI HASSAN BAWA* AND ²ALI HASSAN BAWA

¹Department of Physics, University of Misurata, Misurata, Libya.

²The Bio-Sciences Research and Consultations Office, University of Misurata, Misurata, Libya.
fathiamid17@yahoo.com*

(Received on 27th May 2010, accepted in revised form 3rd March 2012)

Summary: Vibrational spectra have been computed by means of the B3LYP hybrid density functional in order to interpret the experiments [J. Phys. Chem. B 2002, 106, 6358], particularly regarding a transient 1225 cm⁻¹ absorption during accumulation of NO₂ in MgO supported BaO. The degree of generality of results is tested by comparing (NO₂)_x(MO)₉ for x=1, 2 and M=Mg, Ca. Finger prints are produced for the single bidentate M²⁺-[ONO]⁻-M²⁺ surface nitrite ion, a novel single monodentate [O_{clus}-NO₂]²⁻ ion, and the chemisorbed nitrite/nitrate ion pair, i.e., M²⁺-[ONO]⁻-M²⁺+ [O_{clus}-NO₂]²⁻. The results suggest the novel monodentate [O_{clus}-NO₂]²⁻ to be responsible for the experimentally observed 1225 cm⁻¹ absorption, being a transient towards surface nitrate rather than nitrite formation. This result is consistent with a mechanistic periodic DFT study concerning the initial loading of NO₂ in BaO.

Keywords: Density functional theory calculations; (MgO)₉ and (CaO)₉ clusters; Chemisorption; NO₂; Nitrite; Nitrate; Frequency.

Introduction

The cluster concept is at the heart of environmental catalysis technology, as well as its importance in many applied fields of research, such as environmental catalysis [1-3], while providing an efficient means to understand, e.g. deterioration processes. Nitrogen dioxide is one of the most environmental pollutants, primary pollutants are those released directly into the atmosphere from the source in harmful form. Secondary pollutants, by contrast, are modified to hazardous form and then formed by chemical reactions as components of the air mix and interact. Solar radiation often provides the energy for these reactions. Nitrogen oxides are highly reactive gases formed when nitrogen in fuel or combustion air is heated to temperatures above 650 °C in the presence of oxygen. The initial product, nitric oxide (NO), oxidizes further in the atmosphere to nitrogen dioxide (NO₂) [4, 5]. The interest originates mainly from the use of MgO and CaO in "NO_x storage/reduction" catalysts consumption, which has the engine working under lean (oxygen excess) conditions [6]. Under lean conditions

NO is oxidized to NO₂ over the MgO and stored in the form of nitrate or nitrite in the NO_x storing material [7]. The emissions of NO and NO₂ have proved to be very much influenced by operating conditions [8, 9], and many heterogeneous and homogeneous reactions are important for the formation and destruction of NO and NO₂. Vehicle exhaust and other combustion emissions are the main source of nitrogen oxides NO_x, which affect the environment negatively.

The present work attempts to address this issue by examining the NO_x storage mechanism over MgO and CaO clusters by means of quantum chemistry. The setting is provided by experimental and theoretical studies. Experimental input is taken from two investigations on the vibrational spectra of NO_x species observed during calcination of barium nitrate Ba(NO₃)₂(s) [10], and during deposition of NO₂ on MgO supported BaO [11], while very relevant theoretical aspects are found in investigations, which concern the actual NO_x loading mechanism. Key observations are (a) the enhancement in stability observed when molecular NO₂ is added pair-wise to an MgO (001) surface [12], and similar features observed for the BaO (100) substrate [13], which combined provide a possible comprehensive mechanistic understanding of the NO₂ storage in alkaline earth oxides. While these studies are internally consistent and point towards a general understanding, there remain questions regarding the applicability of the computational model as semi-infinite crystal surfaces are taken to model the active catalyst, which suggests that NO_x reacted with B²⁺ to produce barium nitrate Ba(NO₃)₂. A series of alkaline earth oxide cluster studies have been undertaken in order to take this aspect into account. Thus, initial investigation [14] demonstrated how the stabilities of alkaline earth oxide clusters increase with increasing size, and the applicability of the B3LYP hybrid density functional [15-17] for such cluster calculations was tested. In a subsequent study, relative stabilities of isomers were at focus [18], while in a recent comparative study [19], structure and chemisorptions energies of NO₂ was addressed.

*To whom all correspondence should be addressed.

A subsequent study will address the CO₂ (ads), structure and stability at MgO(s) and CaO(s). Two adsorbed NO₂ species were characterized in our previous study [19] by two routes, one corresponding to a surface nitrite, and a second NO₃²⁻ species with sp³ hybridized nitrogen.

The aims of this study is twofold: (a) the enhancement of NO₂(ads) stability upon pair-wise adsorption for alkaline earth oxide clusters is addressed [12,13] taking (MgO)₉ and (CaO)₉ as representatives. It is found that the NO₂ pairwise is energetically much more favourable than the single NO₂, and (b) Significantly, the connection between theoretical and experimental vibration spectra [10, 11] for positive identification of adsorbed species is sought.

Computational Method

The computational procedure employed in the present study follows that outlined in [14, 18, 19], as implemented in the Gaussian 98 program package [20]. Thus the B3LYP hybrid density functional was employed throughout. Indeed, it may be stated that it was precisely in order to produce semi-quantitative results for chemisorptions that this choice was first made. This description of the electronic degrees of freedom has been exploited extensively, as extensive experience has been gained at our laboratory regarding its applicability to small and medium size molecules, and intuition has been developed. This study addresses clusters, and comparatively small basis sets are employed for cost efficiency. This study focuses on the (MgO)₉ and (CaO)₉ clusters. These models of the hexagonal ring stack and slab shaped clusters be good representatives of the corresponding oxide clusters and therefore these were employed to investigate differential properties of (MgO)₉ and (CaO)₉ toward the adsorption of NO₂. The calculations regarding to total energies, bond lengths, angles and vibrational frequencies for isolated NO₂, NO₂⁻, NO₃ and NO₃²⁻ gases as listed in Table- 1, and compared with experiment [21–24]. Very good agreement with measured quantities is obtained. The 6-311G basis sets for B3LYP method are employed for Mg and Ca. In case of the latter, this implies inclusion of one (d) polarization function, and for the N and O atoms, the 6-31+G(d) basis set was used. Vibration spectra were computed from analytical Hessian and validation of possible stationary states on the potential energy surface were made by checking for any imaginary frequencies.

Table-1: Geometries (Å), frequencies (cm⁻¹) and energies (au) for NO₂, NO₂⁻, and NO₃²⁻ calculated at Becke3LYP/6–311G(d) basis set.

Species	R(N–O)	ONO	ω(asym)	ω(sym)	ω(bend)	Energy
NO ₂ ^(a)	1.194	134.2°	1706	1399	766	-205.13271
NO ₂ ^{-(b)}	1.265	115.9°	1303	1364	803	-205.18695
NO ₃ ²⁻	1.259	119.9°	1431	1068	716	-280.42517

^(a) Exp. R(N–O) = 1.193 Å, ∠ONO = 134.1°, ω(asym) = 1618, ω(sym) = 1318, ω(bend) = 750 [21].

^(b) Exp. R(N–O) = 1.236 Å, ∠ONO = 115.4° [22], ω(asym) = 1250, ω(sym) = 1335 [23,24].

Adsorption energies of NO₂ onto the (MgO)₉ and (CaO)₉ cluster models were calculated using the following equation:

$$\Delta E_{\text{ads}} = E(\text{NO}_2) + E(\text{slab, cylinder surface}) - E(\text{NO}_2 \text{ adsorbed surface}) \quad (1)$$

where $E(\text{NO}_2)$ is the energy of a isolated NO₂, $E(\text{slab, cylinder surface})$ is the energy of the optimized (MgO)₉ and (CaO)₉ cluster slab and cylinder and $E(\text{NO}_2 \text{ adsorbed surface})$ is the total energy of adsorbed system.

Results and Discussion

Structural Characteristics of Single and Pairwise NO₂ Adsorption to (MO)_x

In a recent study the chemisorption of NO₂ onto an O_{surf}²⁻ site was described, and particularly the discriminating radical nature NO₂ as adsorbate was emphasized. Two adsorption configurations were investigated for single NO₂ adsorption, corresponding to surface a NO₂⁻ nitrite, and a novel NO₃²⁻ species. The difference between Fig. 1(b) and Fig. 1(c) is the NO₂ binds with two Mg atoms in a bridging bidentate configuration in Fig. 1(b), while NO₂ binds with one oxygen atom in a monodentate configuration in Fig. 1(c). In addition, binding as M²⁺–ONO–M²⁺ forming a surface nitrite can be interpreted as producing an electron vacancy in the O²⁻ ions, i.e. a delocalized O⁻ hole, while the reaction O²⁻–NO₂ was found to localize the odd electron mainly on the adsorbate, resulting in an sp³ hybridized nitrogen. The two surface species are depicted in Fig. 1 and Fig. 2 together with the bare clusters and the pairwise adsorption situation on (MgO)₉ and (CaO)₉ respectively.

It was examined NO₂ pair adsorption behaviour over the (MgO)₉ and (CaO)₉ surface clusters by considering NO₂ binds on cations forming nitrite (NO₂⁻) and NO₂ binds on anions producing nitrates (NO₃⁻). Hence, the addition of second NO₂ causes a pronounced surface relaxation which changed of bond lengths and bond angles, as presented in Table- 2, and the resulting geometries are displayed in Fig. 1(d) and Fig. 2(d) for (MgO)₉ and (CaO)₉ respectively. The structural properties of

the three NO_2 surface species, in order to contrast the structural features of the novel NO_3^{2-} species with the more conventional nitrite and nitrate species found for pairwise adsorption onto the $(\text{MgO})_9$ and $(\text{CaO})_9$ clusters become of interest. The structural parameters are presented in Table- 2. Note, how the $(\text{MgO})_9$ cylinder in Fig. 1 (a) is practically unaltered upon addition of the single NO_2 to form either the NO_3^{2-} or the NO_2^- surface species [see, Fig. 1(b) right and Fig. 1 (c)]. This is in contrast to the formation of the nitrite/nitrate pair [Fig. 1(d)], which completely distorts the oxide cluster. This distortion prevails upon removal of the nitrate like NO_2 (ads) species, leaving the chemisorbed nitrite form [Fig. 1(b) left]. Interestingly, in case of NO_2 adsorption to $(\text{CaO})_9$, the slab shape [Fig. 2(a-d)] of the oxide cluster is preserved throughout.

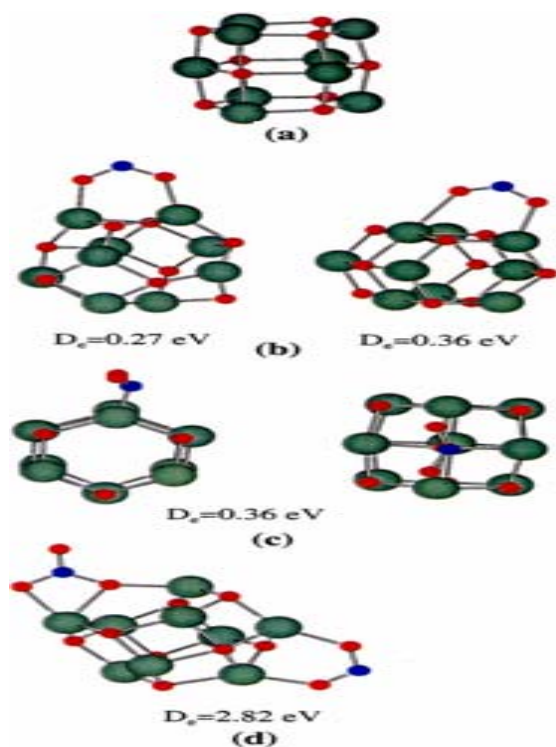


Fig. 1: The optimized structures of (a) the bare $(\text{MgO})_9$ cluster (b) the bidentate nitrite species (c) the NO_3^{2-} species, and (d) the chemisorbed nitrite-nitrate pair at the $(\text{MgO})_9$ cluster are depicted. The degree of cluster distortion in (d) compared to (a) is emphasized, as the tilted geometry in the NO_3^{2-} surface species, indicative of an sp^3 hybridized nitrogen. Oxygen atoms of NO_2 are in red and nitrogen atoms are in blue.

Table-2: Structural parameters^a of nitrite (NO_2^-), nitrates (NO_3^-) and NO_3^{2-} on $(\text{MgO})_9$ and $(\text{CaO})_9$. Compare Fig. 1 and Fig. 2.

Species	R(N-O)	R($\text{NO}_2\text{-M}_{\text{surf}}$)	\angle ONO	\angle ON-M _{surf}	Tilt angle
Nitrite on $(\text{MgO})_9$					
(fig. 1b, right)	a=1.21	a=2.15	124°	$\alpha = 118^\circ$	
	b=1.23	b=2.53		$\beta = 130^\circ$	
	1.27	2.07	117°	128°	
Nitrite on $(\text{CaO})_9$					
(fig. 2b)	a=1.25	a=2.37	115°	$\alpha = 118^\circ$	
	b=1.27	b=2.50		$\beta = 149^\circ$	
(fig. 2d)	a=1.27	a=2.41	115°	$\alpha = 130^\circ$	
	a=1.26	a=2.44		$\beta = 138^\circ$	
NO_3^{2-} on $(\text{MgO})_9$					
(fig. 1c)	1.30	1.45	125°	110°	133°
NO_3^- on $(\text{MgO})_9$					
(fig. 1d)	a=1.27	1.31	125°	$\alpha = 121^\circ$	180°
	b=1.21			$\beta = 114^\circ$	
NO_3^{2-} on $(\text{CaO})_9$					
(fig. 2c)	1.29	1.51	120°	110°	132°
NO_3^- on $(\text{CaO})_9$					
(fig. 2d)	1.24	1.32	125°	118°	180°

^a Bond lengths are in angstroms and angles are in degrees. M=Mg, CaO.

Odd-Even Effect in the Chemisorption Energy of NO_2 to $(\text{MO})_x$, M=Mg, Ca

NO_2 binding energies for the single and pairwise adsorptions are also included in Fig. 1 and Fig. 2. Compared to NO_2 binding energies for the single NO_2 pair adsorption interacts with the $(\text{MgO})_9$ and $(\text{CaO})_9$ clusters more strongly. A striking result for the binding of the second NO_2 molecule comes out significantly more exothermic than the first, i.e. 0.36 eV and 1.66 eV for the initial nitrite formation on $(\text{MgO})_9$ and $(\text{CaO})_9$, respectively, while 2.82 eV and 3.64 eV were obtained respectively for the pairwise adsorption.

It is noted that while the absolute numbers are significantly different, the stabilizations upon adding the second NO_2 are of the same magnitude, i.e. 2.46 eV *versus* 1.98 eV.

The coverage dependence of chemisorption energy was investigated in order to test the generality of this feature. Thus, the evolution of stability upon adding one, two and three CO_2 molecules to form the corresponding carbonates CO_3^{2-} was investigated for a subsequent study.

Hence, it may be concluded that it is the pairing up of the odd electron in the case of adsorption of the NO_2 radical, which results in the enhanced chemical stability of the average NO_2 adsorption energy for the resulting nitrite/nitrate pair.

It is deduced that this effect is similar to what has been known for metal clusters, i.e. a cluster

which having the unpaired electron in the vicinity of the binding site displays a significantly stronger binding to a radical adsorbate than does a cluster, where the electrons are all paired up [25]. In case of the latter, no sink for the extra electron was the cause for the poor binding, which effectively left electron in an anti-bonding cluster orbital. Here, a second NO_2 molecule accepts the excess electron, as a nitrite-nitrate pair is formed.

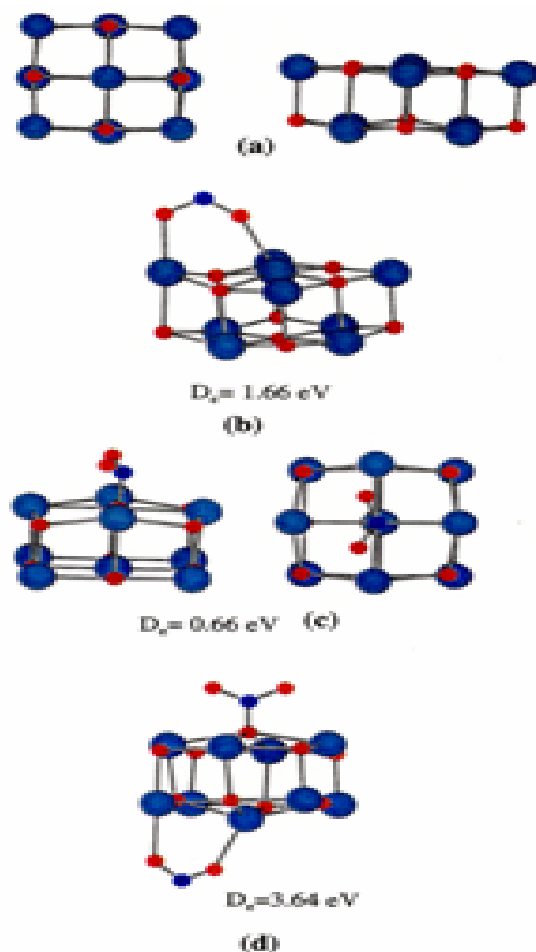


Fig. 2: The optimized structures of (a) the bare $(\text{CaO})_9$ cluster (b) the bidentate nitrite species (c) the NO_3^{2-} species, and (d) the chemisorbed nitrite-nitrate pair at the $(\text{CaO})_9$ cluster are depicted. Note, how the slab shape substrate is conserved throughout (a-d), and the tilted geometry in the NO_3^{2-} surface species, indicative of an sp^3 hybridized nitrogen. The corresponding adsorption energies D_c are showing. Oxygen atoms of NO_2 are in red and nitrogen atoms are in blue.

Vibration Frequency Characteristics of Single and Pairwise NO_2 Adsorption on $(\text{MO})_x$

It is inferred from the above results that energetic and structural properties have been acquired regarding single and pairwise NO_2 adsorption. Here, connection between theoretical predictions and reality are sought by comparing computed and measured vibration spectra. Thus, in Table- 3 the characteristic vibration frequencies are displayed in conjunction with those of the bare clusters. It is noted that the formation of stable the respective NO_3^{2-} , nitrite and nitrate species preserve their integrates irrespective of substrate. Chemisorption on $(\text{MgO})_9$ cluster causes a much more pronounced red shift (441 cm^{-1}) of the asymmetric and weaker red shift (292 cm^{-1}) of the symmetric stretches, so the two bands separated by only 149 cm^{-1} , while at a $(\text{CaO})_9$ cluster (Fig. 2), both modes are further red-shifted by 157 cm^{-1} (Table- 3). This becomes particularly important, in conjunction with the fact that it displays characteristic absorption at 1104 (1113) and 1268 (1269) cm^{-1} on the MgO (CaO) clusters, whereas the nitrites and nitrates produce vibration frequencies at 1363 (1376), 1312 (1317), 791 (792) cm^{-1} and at 1635 (1576), 1317 (1349), 1028 (1028) cm^{-1} , respectively on the Mg_9O_9 (Ca_9O_9) clusters. Hence, neither nitrite nor nitrate displays any vibration frequencies in the window between 1100 and 1300 cm^{-1} , which is precisely where the highest vibration frequencies on the novel NO_3^{2-} species show up.

Table-3: Vibrational frequency ω in cm^{-1} for free NO_2 , the NO_3^{2-} surface species, and the nitrite/nitrate pair on $(\text{MgO})_9$ and $(\text{CaO})_9$ clusters.

Species	$\omega_1(\text{sym})$	$\omega_2(\text{bend})$	$\omega_3(\text{asym})$
NO_2	1396	749	1709
NO_2 on $(\text{MgO})_9$			
NO_3^{2-}	1104	700	1268
NO_2 on $(\text{CaO})_9$		810	
NO_3^{2-}	1113	696	1269
		746	
2(NO_2) on $(\text{MgO})_9$			
NO_2^-	1363	791	1312
NO_3^-	1635	1028(C_{3v})	1317(C_{2v})
		792(C_{2v})	763(C_{2v})
		695(C_{2v})	
2(NO_2) on $(\text{CaO})_9$			
NO_2^-	1376	792	1317
NO_3^-	1349(C_{2v})	792(C_{3v})	1576
	1028(C_{3v})	724(C_s)	
		703(C_{2v})	

Experimentally, two vibration spectroscopy were determined the values of NO_x related compounds on alkaline earth oxides, as property of the lean burn catalyst component BaO . One suggested that in a $\text{Ba}(\text{NO}_3)_2(\text{s})$ calcinations study, the transition between the original compound and the intermediate NO_x related compounds were monitored

by means of Raman Spectroscopy [10]. Frequencies at 1634, 1357–1406, and 1047 cm^{-1} were found to correspond to bulk nitrate. Subsequent measurements during calcinations registered the evolution of a new doublet at 1335 and 1050 cm^{-1} . With the laps of time, a shoulder feature emerged at 1235 cm^{-1} , and this absorption, assigned to a particular nitro species (see, e.g. ref. 10), remained for as long as there was any NO_x left in the sample. It suggested here, that the novel NO_3^{2-} species may very well be the cause of this 1235 cm^{-1} band. And a second is the most relevant study by Hess and Lunsford [11], which monitors the accumulation of NO_2 in MgO supported BaO. During the first 3 minutes of exposure, absorptions at 1327, 1225, and 811 cm^{-1} emerged, suggestive of formation of surface nitrites and NO_3^{2-} species. Subsequently, an additional band at 1051 cm^{-1} emerged, taken to indicate increasing concentrations of nitrates. The final spectrum displayed all the characteristic features of bulk $\text{Ba}(\text{NO}_3)_2$.

Based on the above results that the region of the 1225(1235) cm^{-1} is the novel NO_3^{2-} surface species. At low $\text{NO}_2(\text{ads})$ coverages, this species is expected to coexists with surface nitrites, which in turn would be the cause of the 1327 cm^{-1} absorption band.

Conclusions

A mechanistic understanding of the loading of NO_2 in BaO has previously been presented based on initial nitrite formation, and transient accumulation of nitrite/nitrate pairs. Periodic Density functional theory was employed in order to quantify the relative stabilities of intermediates during this process [11]. This approach and understanding was found to be consistent with interpretations of the NO_2 loading on MgO supported BaO by means of Raman Spectroscopy [13]. Building on investigations regarding inherent properties of alkaline earth oxide clusters [14, 18] in conjunction with claimed understanding of NO_2 to cluster chemisorptions [19], we have addressed here the enhancement in binding energy upon pairwise NO_2 adsorption reported for MgO (001) surface [12]. In addition, the formation of a nitrite/nitrate pair, is strongly with respect to single NO_2 adsorption. The computed in stability for a single adsorbed nitrite is 0.36 eV and (1.66 eV) for Mg_9O_9 (Ca_9O_9), pairs adsorption displays a 2.82 eV (3.64 eV) stability.

Structures of single and pairwise chemisorbed $\text{NO}_2(\text{ads})$ were optimized and vibration frequencies were determined in order to make

connection with experiment, and indeed, the results are in agreement with the experimental interpretations [11] regarding the presence of nitrite and nitrate species. But more than that, an alternative interpretation as to the origin of a 1225 (1235) cm^{-1} band was proposed to correspond to the novel NO_3^{2-} surf surface species [2, 13, 19]. This adsorption is at frequency window where neither nitrite nor nitrate possess any absorptions, while NO_3^{2-} surf displays one at 1268 and 1269 cm^{-1} on the $(\text{MgO})_9$ and $(\text{CaO})_9$ clusters, respectively. The fact that this vibration frequency is fairly independent of oxide cluster cation is taken to infer support for the observation of a novel NO_3^{2-} molecular anion with its own integrity and of general importance. The sp^3 hybridization of N^+ has been assumed in the case of structures [see, Fig. 1(c) and Fig. 2 (c)], leads to bound to three O^- , which stabilized by surrounding cations.

Acknowledgements

The computing facilities at the Department of Inorganic Chemistry, Gothenburg University, Sweden are acknowledged for their assistance.

References

1. M. Miletic, J. L. Gland, K. C. Hass and W. F. Schneider, *Surface Science*, **546**, 75 (2003).
2. L. Cheng and Q. Ge, *Surface Science*, **601**, L65 (2007).
3. S. Abdel Aal, W. S. Abdel Halim and A. S. Shalabi, *Solid State Communications*, **148**, 464 (2008).
4. J. A. Rodriguez, T. Jirsak, J. Y. Kim, J. Z. Larese and A. Maiti, *Chemical Physics Letters*, **330**, 475 (2000).
5. C. D. Valentin, A. Figini and G. Pacchioni, *Surface Science*, **556**, 145 (2004).
6. N. Takahashi, H. T. Iijima, T. Szuki, K. Yamazaki, K. Yokota, H. Suzuki, N. Miyoshi, S. Matsumoto, T. Tanizawa, T. Tanaka, S. Tateishi and K. Kasahara, *Catalysis Today*, **27**, 63 (1996).
7. C. Verrier, J. H. Kwak, D. H. Kim, C. H. F. Peden and J. Szanyi, *Catalysis Today*, **136**, 121 (2008).
8. H. Shinjoh, N. Takahashi, K. Yokota and M. Sugiura, *Applied Catalysis B: Environmental*, **15**, 189 (1998).
9. X. Lu, X. Xu, N. Wang and Q. Zhang, *Journal of Physical Chemistry B*, **103**, 5657 (1999).
10. G. Mestl, M. P. Rosynek, and J. H. Lunsford, *Journal of Physical Chemistry B*, **101**, 9321 (1997).

11. C. Hess and J. H. Lunsford, *Journal of Physical Chemistry B*, **106**, 6358 (2002).
12. W. F. Schneider, K. C. Hass, M. Miletic and J. L. Gland, *Journal of Physical Chemistry B*, **106**, 7405 (2002).
13. P. Broqvist, I. Panas, E. Fridell and H. Persson, *Journal of Physical Chemistry. B*, **106**, 137 (2002).
14. F. Bawa, and I. Panas, *Physical Chemistry Chemical Physics*, **3**, 3042 (2001).
15. A. D. Becke, *Journal of Chemical Physics*, **98**, 5648 (1993).
16. C. Lee, W. Yang and R. G. Parr, *Physical Review B*, **37**, 785 (1988).
17. S. H. Vosko, L. Wilks and M. Nusair, *Canadian Journal of Physics*, **58**, 1200 (1980).
18. F. Bawa, and I. Panas, *Physical Chemistry Chemical Physics*, **4**, 103 (2002).
19. F. H. Bawa, *Journal of the Chemical Society of Pakistan*, **32**, 4 (2010).
20. M. J. Frisch, G. W. Trucks and H. B. Schlegel *et al*, *Gaussian 98*, Gaussian Inc., Pittsburgh, PA (1998).
21. D. R. Lide (Ed.), *C. R. C Handbook of Chemistry and Physics 73RD*, CRC Press, Boca Raton, FL, p. 10 (1992-1993).
22. N. N. Greenwood and A. Earnshaw, *Chemistry of the Elements*, Pergamon Press, Oxford, 1993.
23. K. Nakamoto, *Infrared and Raman Spectra of Inorganic and Coordination Compounds*, Wiley-Interscience, New York (1986).
24. K. M. Ervin, J. Ho and W. C. Lineberger, *Journal of Physical Chemistry*, **92**, 5405 (1988).
25. I. Panas, J. Schule, Siegbahn and U. Wahlgren, *Chemical Physics Letters*, **149**, 265 (1988).